ACTA ABP BIOCHIMICA POLONICA

Vol. 70, No 4/2023
777–784
https://doi.org/10.18388/abp.2020_6254

Regular paper

Circular RNA AGFG1 motivates breast cancer cell proliferation, invasion, migration, and glycolysis by controlling microRNA-653-5p/14-3-3 protein epsilon

Liang Chen[1#], JinXian Qian[1], Ying Shen[3] and Xiang Yu[2#]

[1]Department of Breast Surgery, The First Affiliated Hospital of Kunming Medical University, Kunming City, Yunnan Province, 650032, China; [2]Emergency Trauma Surgery, First People's Hospital of Yunnan Province, Kunming City, Yunnan Province, 650034, China; [3]Department of General Surgery, Yunnan New Kunhua Hospital, Anning City, Yunnan Province, 650301, China

A recent Pairwise meta-analysis confirmed that circular RNA AGFG1 (circAGFG1) is abnormally highly expressed in breast cancer (BC) and may be associated with death risk. The purpose of this study was to elucidate the biological role of circAGFG1 in BC and to explore its potential downstream molecular mechanisms. CircAGFG1, miR-653-5p and YWHAE expression in BC tissues and cells were analyzed by RT-qPCR or western blot. Gene expression was regulated by transfection of plasmids or oligonucleotides and the biological behaviors of BC cells were analyzed by a series of assays. The ring structure of circAGFG1 was analyzed by RNase R and actinomycin D treatment. Dual luciferase reporter assay and RNA-pull down were used to verify the targeting relationship of circAGFG1 and downstream factors. A nude mouse xenograft experiment was performed to verify the effect of circAGFG1 on cancer cells *in vivo*. The results showed that circAGFG1 and YWHAE were highly expressed in BC while miR-653-5p was lowly expressed. Both circAGFG1 and YWHAE had a targeting relationship with miR-653-5p. Knockdown of circAGFG1 inhibited BC cell proliferation, invasion, migration, and glycolysis. The inhibitory effect of circAGFG1 knockdown on BC was reversed by silencing miR-653-5p. The inhibitory effect of overexpression of miR-653-5p on malignant behaviors of BC cells was reversed by overexpression of YWHAE. Knockdown of circAGFG1 inhibited tumor growth *in vivo*. Taken together, these data suggest that circAGFG1 acts as a sponge for miR-653-5p to mediate YWHAE expression to promote the malignant behaviors of BC.

Keywords: Circular RNA AGFG1, MicroRNA-653-5p,YWHAE, Target binding, MDA-MB-231 cells

Received: 05 March, 2022; revised: 29 July, 2023; accepted: 16 August, 2023; available on-line: 18 October, 2023

e-mail: qianjx2000@hotmail.com (JXQ); yxiang56@163.com (YS)
#These authors contributed equally to this work.:

INTRODUCTION

Breast cancer (BC) is a malignant tumor in the mammary gland epithelial tissue, which seriously threatens the survival and health of women worldwide (Wang *et al*., 2021). Surgery, endocrine therapy, chemotherapy, radiotherapy and targeted therapy are applicable for BC treatment to reduce the mortality rate (Li *et al*., 2021). However, due to high recurrence and easy metastasis, patients' prognosis is still poor, and the mortality rate is still high (Xie *et al*., 2021). Hence, an in-depth study of the latent molecular mechanisms of BC is crucial to provide new and effective therapeutic targets.

Circular RNAs (circRNAs) are a cluster of closed circular RNAs (Li *et al*., 2019). A study has shown that circRNAs are available to control gene expression and the biological behavior of cancer cells (Wu *et al*., 2019). Meanwhile, multiple circRNAs have been revealed to take part in regulating BC progression (Zhang *et al*., 2021; Qi *et al*., 2021; Cui *et al*., 2021). CircAGFG1 is a novel circRNA that has been confirmed to be elevated in BC and may be implicated in the diagnosis and prognosis of BC (Ma *et al*., 2021). However, it is unclear whether circAGFG1 affects the biological behavior of BC cells.

circRNAs can perform as competing endogenous RNAs (ceRNAs) for microRNAs (miRNAs) to control downstream targets (Chu *et al*., 2021). In the light of the ceRNA theory, it predicted a miRNA (miR-653-5p) associated with circAGFG1. Recently, miR-653-5p has been tested to involve diversified cancers, such as non-small cell lung cancer (Han *et al*., 2019) and gastric cancer (Li *et al*., 2021). However, it is necessary to further elucidate other downstream target genes regulated by miR-653-5p in BC.

YWHAE, also known as 14-3-3ε, is a member of the YWHA protein family (Wu *et al*., 2021). YWHAE which is extensively expressed in most cancers is a transcription factor [(Li *et al*., 2021). Previous studies have shown that YWHAE is elevated in BC and can motivate the proliferation, metastasis and chemotherapy of BC cells, and may become a latent therapeutic target for BC (Leal *et al*., 2016; Cimino *et al*., 2008; Park *et al*., 2019).

This study hypothesized that circAGFG1 might indirectly regulate YWHAE expression by adsorbing miR-653-5p to participate in BC cell biological behaviors. Our aim was to explore the biological function of circAGFG1 in BC and to elucidate its downstream underlying mechanisms.

MATERIALS AND METHODS

Clinical tissue specimens

From January 2018 to January 2020, BC tissues and adjacent normal tissues (2–5 cm from the tumor) of 60 patients (aged 47.5±11.4 years) who underwent tumor resection at The First Affiliated Hospital of Kunming Medical University were harvested. All tissues were stored at –80°C. Approval of this study was obtained from the Ethics Committee of The First Affiliated Hos-

pital of Kunming Medical University and written informed consent was collected from all participants.

Cell culture and transfection

Normal human breast cells (MCF-10A) and human BC cell lines (MDA-MB-231, MCF-7, SK-BR-3 and MDA-MB-157) were bought from ATCC (VA, USA). The cells were cultivated in Roswell Park Memorial Institute-1640 (31800, Solarbio, China) containing 10% fetal bovine serum at 37°C, and 5% CO_2. MDA-MB-231 cells were chosen as an auxiliary study object because they had the greatest difference in expression (Yang *et al*., 2019).

Specific short hairpin RNAs against circAGFG1, miR-653-5p mimic/inhibitor, and corresponding NCs were gained from Genepharma (Shanghai, China). Lentivirus-negative vector, YWHAE and circAGFG1 lentiviral overexpression vectors were purchased from GeneCopoeia. MDA-MB-231 and MDA-MB-157 cells were transferred to a 6-well plate (1×10^5 cells/mL) and cultured for 24 h. Cell transfection was conducted using Lipofectamine® 2000 (Invitrogen, USA) (Gong *et al*., 2021). 48 h after transfection, the transfection efficiency was evaluated by reverse transcription-quantitative polymerase chain reaction (RT-qPCR) and Western blot.

Ribonuclease R (RNase R) and actinomycin D

To test RNase R resistance, total RNA (2 μg) from MDA-MB-231 cells was collected and incubated with 3 U/μg RNase-R (07250, Epicentre Technologies, USA) at 37°C for 30 min. Actinomycin D experiment: MDA-MB-231 cells were treated with 2 mg/mL actinomycin D (129,935, Millipore, USA) to block transcription. Then, cellular RNA was obtained to measure circAGFG1 and AGFG1 expression by RT-qPCR.

Subcellular localization analysis

Cytoplasmic and nuclear RNAs of MDA-MB-231 cells were isolated using the PARIS Kit (Invitrogen). Then, circAGFG1 in cytoplasmic RNA and nuclear RNA was checked by RT-qPCR. U6 and glyceraldehyde-3-phosphate dehydrogenase (GAPDH) were applied as nuclear and cytoplasmic controls, respectively.

RT-qPCR

Total RNA was extracted from BC tissues and cells using Trizol reagent (Invitrogen) PrimeScript RT reagent kit (Takara, Tokyo, Japan) and miRNA First Strand Synthesis kit (Takara, Japan) were employed for reverse transcription of circRNA/mRNA and miRNA, respectively. RT-qPCR was performed with SYBR Green kit (Thermo Fisher Scientific, MA, USA) and Mx3005P QPCR system (Agilent Technologies, Santa Clara, CA, USA). U6 and GAPDH were employed as internal controls for miRNA and mRNA/circRNA, respectively (Ma *et al*., 2021). The primer sequences were manifested in Table 1. The relative expression of genes was analyzed by $2^{-\Delta\Delta Ct}$.

Western blot

Total protein from cells and tissues was extracted with 500 μL radio-immunoprecipitation assay lysis buffer (Beyotime). An equal amount of protein (20 μg) was separated by 8% sodium dodecyl sulfate-polyacrylamide gel electrophoresis (Solarbio) and transferred to a polyvinylidene fluoride membrane (Invitrogen). After being blocked with 5% skim milk, the membrane was incubated with primary antibodies YWHAB (8312, Cell Signaling Technology, 1:1000), glucose transporter type1 (GLUT1; ab652, 1:1000), matrix metalloproteinase-9 (MMP9; ab38898, 1:1000), B cell lymphoma 2-associated X (Bax; ab32503, 1: 1000, all Abcam), and GAPDH (60004-1-Ig, 1:1000, Proteintech) overnight at 4°C. Horseradish peroxidase-conjugated goat anti-rabbit secondary antibody immunoglobulin G (1:1000, ab181236, Abcam) was added for incubation for 2 h. The signals were visualized by an enhanced chemiluminescence kit (34080, Thermo Fisher Scientific) and analyzed by ImageJ software. Three biological replicates of the experiment were performed.

Table 1. Primer sequence

Genes	Primer sequence (5′-3′)
CircAGFG1	F: 5′-CCAGTTGTAGGTCGTTCTCAAG-3′
	R: 5′-TCACCCTGTGTGGTGGAT-3′
miR-653-5p	F: 5′-GCCGAGGTGTTGAAACAATC-3′
	R: 5′- TGGTGTCGTGGAGTCG -3′
YWHAE	F: 5′-GGATACGCTGAGTGAAGAAAGC-3′
	R: 5′-TATTCTGCTCTTCACCGTCACC-3′
U6	F: 5′-CTCGCTTCGGCAGCACA-3′
	R: 5′-AACGCTTCACGAATTTGCGT-3′
GAPDH	F: 5′-TCCCATCACCATCTTCCA-3′
	R: 5′-CATCACGCCACAGTTTTCC-3′

F, forward; R, reverse

Cell Counting Kit -8 (CCK-8)

MDA-MB-231 and MDA-MB-157 cells after transfection were seeded in 96-well plates (1×10^4 cells/well). At designated time points (0, 24, 48 h), 10 μL CCK-8 reagent (Dojindo, Kumamoto, Japan) was added to each well. Optical density values at 450 nm were recorded after 2 h on a microplate reader (PerkinElmer, USA).

Colony formation assay

MDA-MB-231 and MDA-MB-157 cells after transfection were seeded in 6-well plates for 14 d, fixed in 4% paraformaldehyde (Beyotime), stained with 0.1% crystal violet (Beyotime) for 2 h, and counted.

Flow cytometry

Apoptosis rates of transfected MDA-MB-231 and MDA-MB-157 cells were analyzed by Annexin V-Fluorescein isothiocyanate (FITC) propidium iodide (PI) apoptosis kit (BD Biosciences). Briefly, cells were resuspended in 1 × binding buffer (500 μl) and mixed with 5 μl Annexin V-FITC and 5 μl PI in the dark for 15 min. Finally, the percentage of apoptotic cells was evaluated by a flow cytometer (FACS Calibur).

Transwell migration and invasion analysis

MDA-MB-231 and MDA-MB-157 cells were placed in a serum-free medium at a density of 5×10^4 cells/well, and the medium containing 10% fetal bovine serum (Invitrogen) was added to the bottom chamber. Then after 24 h, cells were fixed with methanol for 30 min, stained with 0.1% crystal violet, and viewed in an inverted mi-

croscope (Tycom, Switzerland, magnification ×100). For invasion assays, cells (1×10^6 cells/well) were placed in the upper chamber (Costar) coated with a matrix (BD Bioscience) (Wan *et al.*, 2021).

Glycolysis test

MDA-MB-231 and MDA-MB-157 cells (1×10^5 cells/well) after transfection were seeded in 12-well plates. After 48 h of transfection, glucose consumption, and lactate production, the ADP/ATP ratio were tested using a glucose detection kit (Sigma-Aldrich), a lactate detection kit (BioVision, Milpitas, CA, USA), and a carrier sensor ADP/ATP ratio detection kit (BioVision), respectively (Xie *et al.*, 2021).

The luciferase activity assay

MDA-MB-231 cells were plated on 6-well plates and then co-transfected with the luciferase reporters pRL-TK-CircAGFG1/YWHAE-WT 3-UTR or pRL-TK-CircAGFG1/YWHAE-MUT 3-UTR (Promega), and miR-653-5p mimic or mimic-NC using Lipofectamine®2000 (Invitrogen). After 48-h incubation, luciferase activity was measured using a dual luciferase reporter gene kit (Promega) (Wu *et al.*, 2021).

RNA-pull down assay

Biotin-labeled miR-653-5p (Bio-miR-653-5p) probe and control probe (Bio-NC) were gained from RiboBio. After transfection with Bio-NC or Bio-miR-653-5p, MDA-MB-231 cells were lysed after 48 h and incubated with Dynabeads M-280 Streptavidin (Invitrogen) at 4°C for 2 h. The RNA complexes on the beads were washed and the enrichment of circAGFG1 and YWHAE was tested by RT-qPCR.

In vivo tumor growth assay

Twelve BALB/c male nude mice (5 weeks old, body weight of 15–20 g) were purchased from Vital River (Beijing, China). MDA-MB-231 cells (5×10^6 cells/mouse) with or without stable knockdown of circAGFG1 were injected subcutaneously into each mouse (6 per group). Tumor volume was calculated in the light of the formula $0.5\times\text{length}\times\text{width}^2$ and measured every 3 d. After 23 d, the mice were euthanized. Tumor tissues were excised for further analysis. This study was permitted by the Animal Research Committee of The First Affiliated Hospital of Kunming Medical University (Ding *et al.*, 2021).

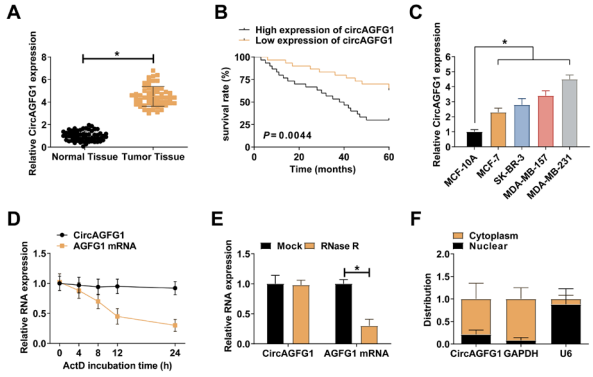

Figure 1. CircAGFG1 is elevated in BC
(**A**) RT-qPCR detection of circAGFG1 in normal and tumor tissues. (**B**) Kaplan-Meier analysis of survival prognosis of BC patients. (**C**) RT-qPCR detection of circAGFG1 expression in four BC cell lines (MDA-MB-231, MCF-7, SK-BR-3, and MDA-MB-157) and normal breast cell line (MCF-10A) (**D/E**) The ring structure of circAGFG1 was determined by RNase R and Act D methods. (**F**) The subcellular localization of circAGFG1 in MDA-MB-231 cells. Measurement data were clarified as mean ± S.D. (N=3); *P<0.05.

Immunohistochemistry (IHC) analysis

After being fixed in 10% formalin (Beyotime), the tumor tissues were embedded in paraffin and dissected. Primary antibodies Ki67 (ab15580, 1:5000, Abcam, Cambridge, UK) and MMP9 (ab76003, 1:1000, Abcam) were

Table 2. The link of circAGFG1 and clinicopathological features of BC patients

Characteristic	Cases	CircAGFG1 expression		*P*
	n=60	Reduction (n=30)	Elevation (n=30)	
Age (years)				
<50	27	12	15	0.512
≥50	33	18	15	
Tumor size				
<2cm	35	19	16	0.0357*
≥2cm	25	11	14	
TNM				
I/II	29	19	10	0.0157*
II/IV	31	11	20	
Lymph node metastasis				
Negative	25	17	8	0.0076*
Positive	35	13	22	
Distant metastasis				
No	50	30	20	0.0257*
Yes	10	0	10	

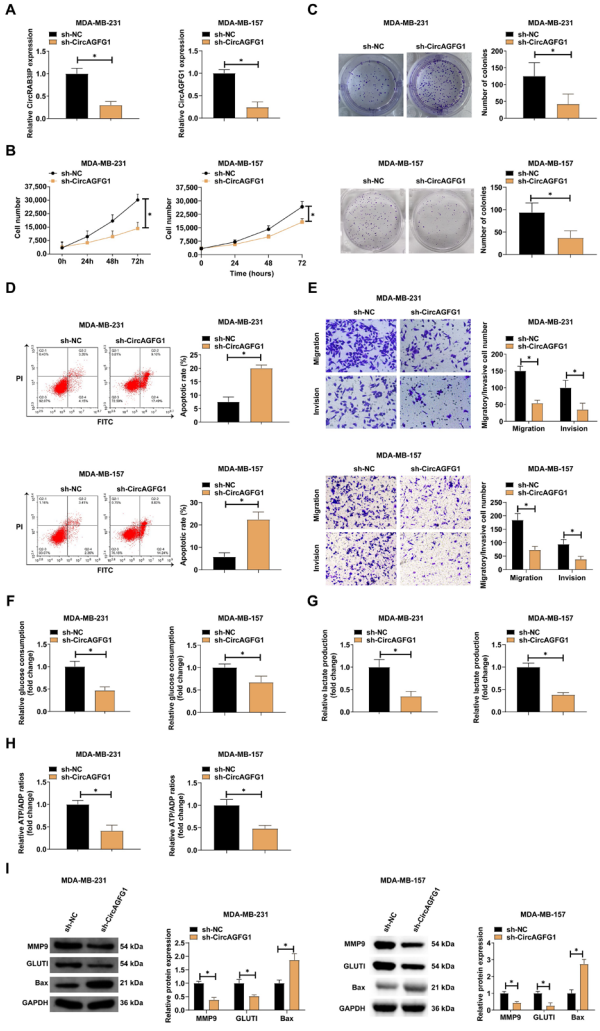

Figure 2. circAGAP1 regulates BC cell proliferation, invasion and migration, glycolysis and apoptosis
sh-circAGFG1 was transfected into MDA-MB-231 and MDA-MB-157 cells. (**A**) RT-qPCR detection of circAGFG1 knockdown or overexpression transfection efficiency. (**B/C**) Cell proliferation activity was tested by the CCK-8 method and colony formation assay. (**D**) Cell apoptosis detected by flow cytometry. (**G**) Transwell assay to measure cell migration and invasion. (**F–H**) glucose consumption, lactate production, and cellular ATP/ADP ratio. I. Western blot detection of GLUT1, Bax, and MMP9. Measurement data were clarified as mean ± S.D. (N=3); *P<0.05.

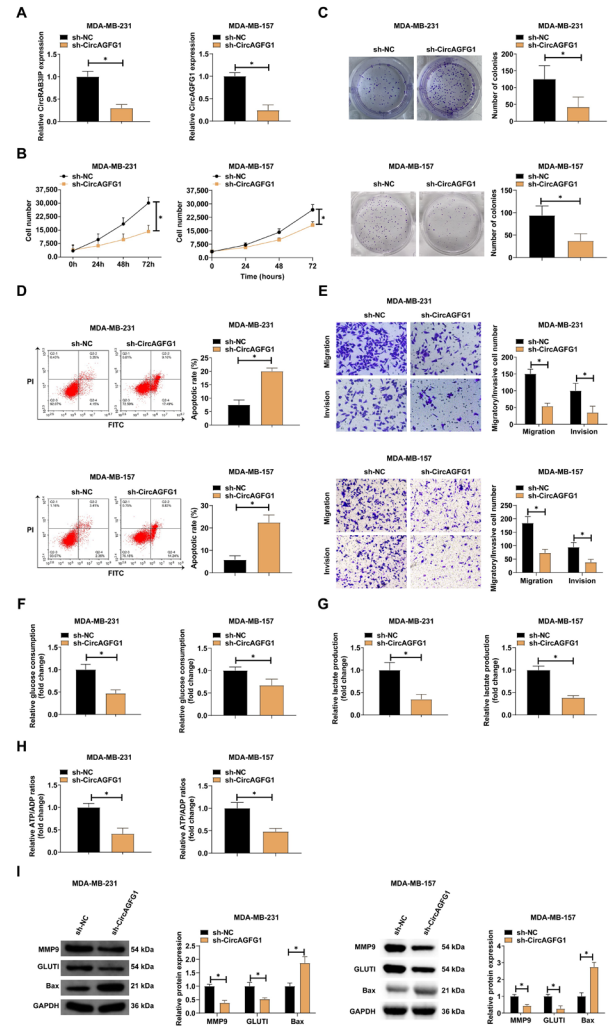

Figure 3. CircAGFG1 acts as a sponge of miR-653-5p
(**A**) The binding sites between circAGFG1 and miR-653-5p on the starbase. (**B**) RT-qPCR detection of transfection efficiency of miR-653-5p mimic. (**C–D**) Luciferase activity assay and RNA-pull down assay to evaluate the interaction between circAGFG1 and miR-653-5p. (**E–F**) RT-qPCR to examine miR-653-5p in BC tissues and cells. (**G**) Pearson correlation analysis to evaluate the correlation between miR-653-5p and circAGFG1. (**H**) RT-qPCR detection of miR-653-5p expression after transfection of sh-circAGFG1. Measurement data were clarified as mean ± S.D. (N=3); *P<0.05.

incubated at 4°C overnight, followed by the secondary antibody (ab205718, 1:5000, Abcam) overnight. After treatment with 3,3'-diaminobenzidine staining (Sangon Biotech, Shanghai, China), the sections were counterstained with hematoxylin (Beyotime) and examined with a fluorescence microscope (Leica, Wetzlar, Germany).

Statistical analysis

All experiments in this study were biologically replicated at least three times. SPSS 21.0 (SPSS, Inc, Chicago, IL, USA) statistical software was applied for analysis of the data. After the Kolmogorov-Smirnov test, the data were normally distributed and expressed as mean ± standard deviation (S.D.). The two-group comparison was done by t-test, while the multiple-group comparison was performed by one-way analysis of variance (ANOVA) and Fisher's least significant difference t-test (LSD-t). The chi-square test was used to analyze the correlation between circAGFG1 and the clinicopathological data of patients and Kaplan-Meier analysis to examine the relationship between circAGFG1 and patients' survival P<0.05 was considered statistically significant.

RESULTS

CircAGFG1 is elevated in BC

Firstly, the circAGFG1 expression pattern in BC was detected by RT-qPCR. CircAGFG1 expression was higher in BC tissues compared with normal tissues (Fig. 1A). The link between circAGFG1 and clinicopathological characteristics of BC patients was then analyzed. The elevation of circAGFG1 was associated with tumor-node-metastasis stage, tumor size, lymph

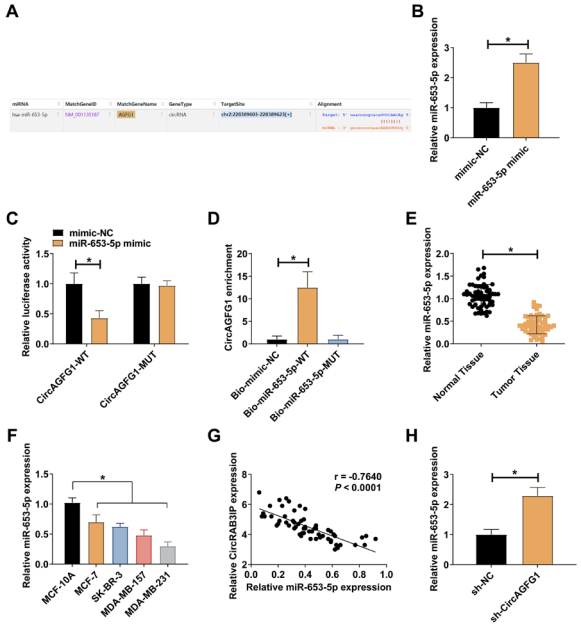

Figure 4. Repression of miR-653-5p reverses the effects of circAGFG1 knockdown on BC cells
sh-circAGFG1 and miR-653-5p inhibitor were co-transfected into MDA-MB-231 and MDA-MB-157 cells. (**A**) The transfection efficiency of sh-circAGFG1 and miR-653-5p inhibitor detected by RT-qPCR. (**B–C**) Cell proliferation activity detected by the CCK-8 method and colony formation assay. (**D**) Apoptosis rate detected by flow cytometry. (**E**) Transwell detection of cell migration and invasion. (**F–H**) Glucose consumption, lactate production, and cellular ATP/ADP ratio. (**I**) Western blot detection of GLUT1, Bax, and MMP9. Measurement data were clarified as mean ± S.D. (N=3); *P<0.05.

node metastasis and distant metastasis, but not with age (Table 2). Kaplan-Meier survival analysis clarified that the elevation of circAGFG1 was associated with worse overall survival (Fig. 1B).

CircAGFG1 expression was higher in all BC cell lines (MDA-MB-231, MCF-7, SK-BR-3, and MDA-MB-157) than in normal cells (MCF-10A) (Fig. 1C). Among them, MDA-MB-231 cells and MDA-MB-157 cells with the highest CircAGFG1 expression were selected for follow-up experiments. The circular structure of circAGFG1 was confirmed by RNase R and actinomycin D experiments, and it came out that circAGFG1 was resistant to RNase R digestion and was more stable than linear AGFG1 mRNA, and actinomycin D did not affect the stability of circAGFG1 (Fig. 1D, E). Furthermore, subcellular localization analysis clarified that circAGFG1 was majorly distributed in the cytoplasm of MDA-MB-231 cells (Fig. 1F).

The above data suggest circAGFG1 is stably elevated in BC and may take part in BC progression.

Repressing circAGFG1 restrains MDA-MB-231 cell biological behaviors and glycolysis

To figure out circAGFG1's biological function in BC, circAGFG1 was silenced in MDA-MB-231 and MDA-MB-157 cells. CircAGFG1 knockdown efficiency was shown in Fig. 2A. CCK-8 and colony formation experiments showed that the knockdown of circAGFG1 inhibited the proliferation ability of BC cells (Fig. 2B, C). Flow cytometry showed that the knockdown of circAGFG1 promoted apoptosis in cells (Fig. 2D). Transwell experiments demonstrated that the knockdown of circAGFG1 increased the migratory and invasive abilities of cells (Fig. 2E). Most fast-growing malignant cells have active glycolysis and gain more energy through glycolysis (Zhang *et al.*, 2022). Next, the effect of circAGFG1 on glycolysis was explored. It was examined that knockdown of circAGFG1 inhibited cellular glucose consumption, lactate production and ATP/ADP ratio (Fig. 2F-H). Western blot detected that knockdown of circAGFG1 suppressed the protein expression of MMP9 and GLUT1 and promoted the protein expression of Bax (Fig. 2I). The above data indicated that knockdown of circAGFG1 refrains BC cell biological functions and glycolysis.

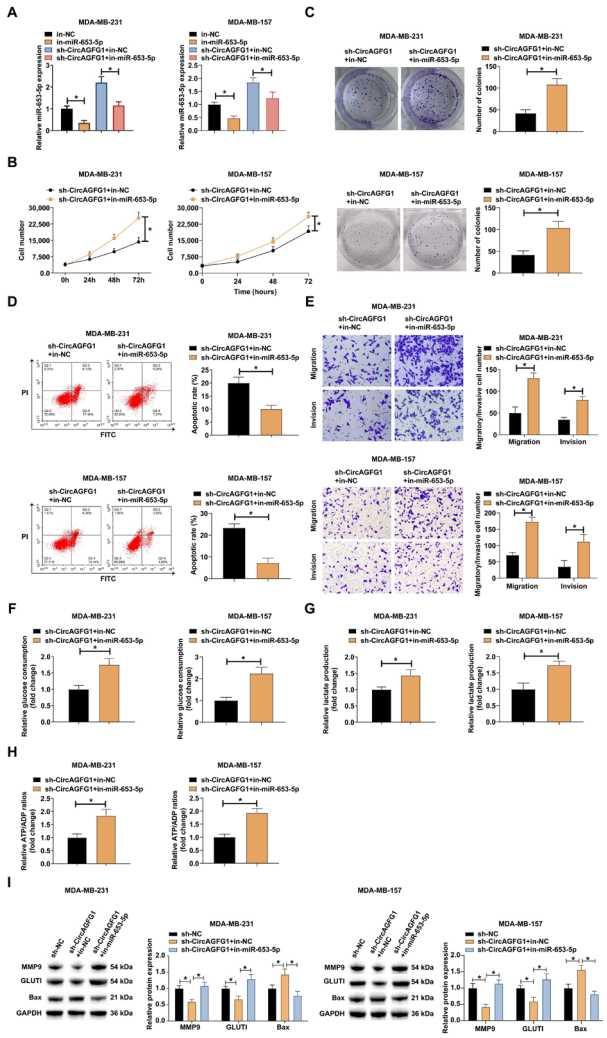

Figure 5. YWHAE is a functional target of miR-653-5p in BC cells
(**A**) Binding sites of YWHAE with miR-653-5p. (**B–C**) The luciferase activity assay and RNA-pull down assay to evaluate the interaction between YWHAE and miR-653-5p. (**D–E**) mRNA expression of YWHAE in BC tissues and adjacent normal tissues detected by RT-qPCR and western blot. (**F–G**) YWHAE expression in four BC cell lines (MDA-MB-231, MCF-7, SK-BR-3 and MDA-MB-157) and a normal breast cell line (MCF-10A) detected by RT-qPCR and western blot. (**H–I**) The correlation among YWHAE, miR-653-5p, and circAGFG1 evaluated by Pearson correlation analysis. (**J**) Western blot detection of YWHAE expression after transfection of sh-CircAGFG1 or miR-653-5p mimic. Measurement data were clarified as mean ± S.D. (N=3); *P<0.05.

CircAGFG1 performs as a sponge for miR-653-5p

circAGFG1 can target miRNAs to regulate BC progression (Qi *et al.*, 2015), so a bioinformatics website

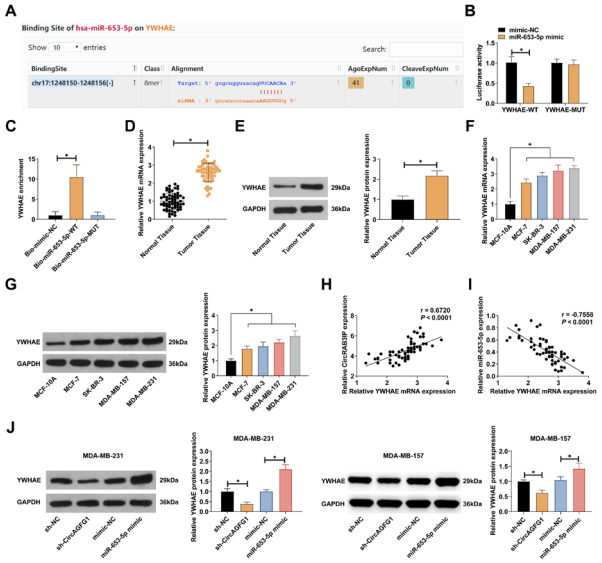

Figure 6. Elevation of miR-653-5p restrains BC cell effect via targeting YWHAE
miR-653-5p mimic and YWHAE overexpression vector were co-transfected into MDA-MB-231 and MDA-MB-157 cells. (**A–B**) RT-qPCR and Western blot examination of YWHAE in MDA-MB-231 cells. (**C–D**) Cell proliferation activity was detected by the CCK-8 method and colony formation assay. (**E**) Cell apoptosis rate tested by flow cytometry. (**F**) Transwell detection of cell migration and invasion. (**G–I**) Glucose consumption, lactate production, and cellular ATP/ADP ratio. (**J**) Western blot detection of GLUT1, Bax, and MMP9. Measurement data were clarified as mean ± S.D. (N=3); **P*<0.05.

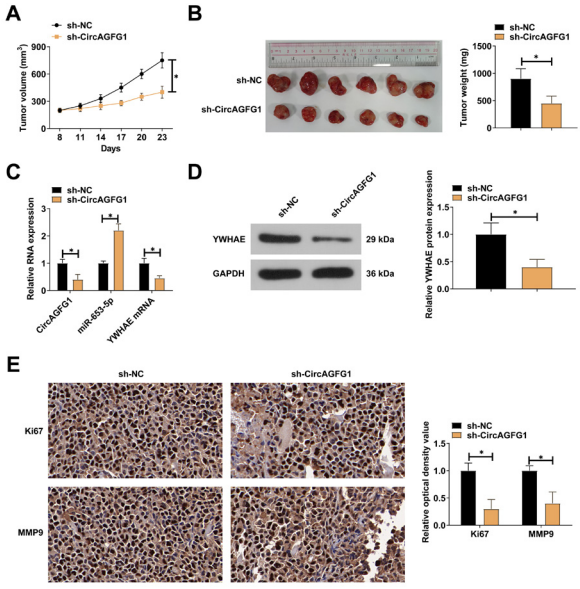

Figure 7. Deletion of circAGFG1 restrains tumorigenesis in vivo
(**A**) Changes in tumor volume in mice. (**B**) The tumor weight of mice was detected after 23 days. (**C**) RT-qPCR to test circAGFG1 and miR-653-5p in tumor tissues. (**D**) Western blot to test YWHAE in tumor tissue. (**E**) Ki67 and MMP9 in tumor tissue detected by IHC. Measurement data were clarified as mean ± S.D. (n=6); **P*<0.05.

(https://starbase.sysu.edu.cn) was utilized to predict the target miRNAs of circAGFG1. In Fig. 3A, miR-653-5p had a targeted binding site for circAGFG1. miR-653-5p mimic elevated miR-653-5p expression in MDA-MB-231 cells (Fig. 3B). Dual luciferase reporter gene test results showed that miR-653-5p mimic restrained the luciferase activity of circAGFG1-WT, but not that of circAGFG1-MUT (Fig. 3C). RNA-pull down assay found that miR-653-5p could specifically combine with circAGFG1 (Fig. 3D). Meanwhile, miR-653-5p expression was reduced in BC tissues and cells (Fig. 3E, F). Clinical correlation analysis found that miR-653-5p was negatively linked with circAGFG1 expression (Fig. 3G). RT-qPCR found that depression of circAGFG1 enhanced miR-653-5p expression in MDA-MB-231 cells (Fig. 3H).

All in all, miR-653-5p is regulated by circAGFG1.

Repression of miR-653-5p reverses the effects of silencing circAGFG1 on BC cells

To further study the role of CircAGFG1 in regulating the expression of miR-653-5p in BC, rescue experiments were executed. The promotion of miR-653-5p by sh-CircAGFG1 was reversed by miR-653-5p inhibitor (Fig. 4A). Colony formation and CCK-8 experiments showed that miR-653-5p inhibitor eliminated the inhibition of sh-circAGFG1 on cell proliferation (Fig. 4B, C). Flow cytometry showed that the proapoptotic effect of sh-circAGFG1 was reversed by miR-653-5p inhibitor (Fig. 4D). Transwell assay showed that sh-circAGFG1 inhibited cell invasion and migration, while miR-653-5p inhibitor prevented this change (Fig. 4E). Detection of glycolysis-related indicators showed that sh-circAGFG1 reduced glucose consumption, lactate production, and ATP/ADP ratio, but this phenomenon was reversed by miR-653-5p inhibitor (Fig. 4F–H). In addition, sh-circAGFG1 inhibited MMP9 and GLUT1 expression and promoted Bax expression, while miR-653-5p inhibitor blocked these protein changes (Fig. 4I).

The above data suggest that circAGFG1 affects BC cell progression *via* targeting miR-653-5p.

YWHAE is a functional target of miR-653-5p in BC cells

Bioinformatics analysis on https://starbase.sysu.edu.cn found the multiple complementary binding sites in miR-653-5p and YWHAE (Fig. 5A). It turned out that miR-653-5p mimic effectively suppressed the luciferase activity of YWHAE-WT 3'UTR (Fig. 5B). Verified by RNA-pull down assay, YWHAE could specifically combine with miR-653-5p (Fig. 5C). The elevation of YWHAE expression was discovered in BC tissues and cells (Fig. 5D-G). Clinical correlation analysis found that YWHAE expression was positively linked with circAGFG1 expression and negatively associated with miR-653-5p expression (Fig. 5H, I). Furthermore, in MDA-MB-231 cells, down-regulation of circAGFG1 or enhancement of miR-653-5p reduced YWHAE expression (Fig. 5J).

The above data indicate that YWHAE is the downstream gene of miR-653-5p.

Elevation of miR-653-5p depresses BC cell effects *via* targeting YWHAE

For further investigating the link between miR-653-5p and YWHAE, a functional rescue experiment was performed. YWHAE expression was significantly increased after transfection of the YWHAE overexpression vector, and the inhibitory effect of miR-653-5p mimic on YWHAE was reversed by the YWHAE overexpression vector (Fig. 6A, B). CCK-8 and colony formation experiments showed that the inhibitory effect of overexpression of miR-653-5p on cell proliferation was reversed by overexpression of YWHAE (Fig. 6C, D). In addition, the promoting effect of overexpression of miR-653-5p on apoptosis was reversed by overexpression of YWHAE (Fig.

6E). Transwell experiments showed that overexpression of miR-653-5p inhibited cell invasion and migration, but overexpression of YWHAE prevented this phenomenon (Fig. 6F). Commercial kit results showed that the inhibitory effects of overexpression of miR-653-5p on cellular glucose consumption, lactate production, and ATP/ADP ratio were reversed by overexpression of YWHAE (Fig. 6G–I). Western blot showed that overexpression of miR-653-5p inhibited the expression of MMP9, GLUT1 and promoted the expression of Bax, and overexpression of YWHAE reversed the changes of these proteins (Fig. 6J).

The above data suggest that miR-653-5p affects BC cell progression by targeting YWHAE.

CircAGFG1 knockdown restrains tumor growth *in vivo*

To determine whether circAGFG1 silencing restrained tumor growth *in vivo*, sh-NC or sh-CircAGFG1-transfected MDA-MB-231 cells were implanted into nude mice. sh-CircAGFG1 reduced the tumor volume and weight of mice (Fig. 7A, B). Meanwhile, circAGFG1 knockdown suppressed circAGFG1 and YWHAE expression in tumor tissues, while elevated miR-653-5p expression (Fig. 7C, D). IHC analysis illustrated that repression of circAGFG1 repressed Ki67 and MMP9 expression in tumor tissues (Fig. 7E). All in all, it is suggested that circAGFG1 knockdown restrains BC tumor growth *in vivo*.

DISCUSSION

BC is an extremely familiar cancer worldwide and a momentous cause of death in women. Its high morbidity, high recurrence rate and unpleasing prognosis are the main reasons of patient death. Hence, in-depth studies of the molecular mechanisms of BC are urgently needed to confirm effective targets for BC therapy. With the in-depth research on regulatory mechanism in cancer, the study direction has gradually shifted from coding RNA to ncRNAs. BC development is complexly controlled by diversified ncRNAs, including circRNAs, and miRNAs (Liu *et al*., 2021). In the research, it was discovered for the first time that circAGFG1 combined with miR-653-5p, which targeted YWHAE, thereby facilitating MDA-MB-231 cell biological behaviors and glycolysis *in vitro* and accelerating tumor growth *in vivo*.

CircAGFG1 has been confirmed to be elevated in BC and may be implicated in BC patients' diagnosis and prognosis. A study has shown that circRNAs are more stable in tissues and exosomes compared with traditional linear RNAs (He *et al*., 2021). Likewise, in the research, circAGFG1 expression was elevated in BC, was not easily degraded by RNase R and was abundantly exhibited in the cytoplasm. In addition, this study also found that circAGFG1 elevation was associated with poor pathological features and prognosis of BC patients. CircAGFG1 expression is enhanced in various cancers like esophageal cancer (Fu *et al*., 2021), cervical cancer, and triple-negative BC (Zhang *et al*., 2021), and repressing its expression can restrain the malignant progression of cancer. In the research, the knockdown of circAGFG1 restrained BC cell biological behaviors and glycolysis, and depressed tumor growth *in vivo*. This suggests that circAGFG1 may offer a therapeutic target for BC. It has been reported that cells can secrete circRNAs through exosomes to regulate tumor growth and metastasis. As exampled, in BC, has_circ_0000615 is packaged by exosomes and transported into the circulating blood (Mashouri *et al*., 2019). Therefore, subsequent studies need to detect BC cell exosomes to detect the role of circAGFG1.

CircRNAs perform as ceRNAs to interact miRNAs. Through bioinformatics analysis, it was found that CircAGFG1 can sponge various miRNAs. Among these miRNAs, miR-653-5p was selected as circAGFG1's target in the research. Elevation of miR-653-5p refrains the proliferation and migration of melanoma (Liu *et al*., 2020), together with the proliferation of cervical cancer cells (Wu *et al*., 2020). MiR-653-5p's functions in BC have been initially clarified, and this miRNA is lowly expressed in BC and has anti-tumor effects. In the research, miR-653-5p expression was inhibited in BC. Furthermore, miR-653-5p inhibitor could partially suppress the effects of circAGFG1 silencing on BC cells.

YWHAE acts as a transcription factor to activate or depress the transcription of target genes. For example, targeting YWHAE to activate apoptotic signaling can suppress cutaneous squamous cell carcinoma (Holmes *et al*., 2021). Previous studies have shown that YWHAE is elevated in BC and motivates the metastasis and chemotherapy of BC cells, and may become a latent therapeutic target for BC. However, the mechanism by which the circAGFG1/miR-653-5p/YWHAE axis affects BC has not been investigated. In the research, it was also found that YWHAE expression was elevated in BC. In addition, it was originally discovered that YWHAE was a downstream gene of miR-653-5p. Meanwhile, YWHAE can integrate multiple signaling pathways by interacting with different proteins in cancer progression (Ou *et al*., 2021). In addition, YWHAE-NUTM2 has been reported to deregulate both v-raf-leukemia viral oncogene 1/v-Raf murine sarcoma viral oncogene homolog B and Hippo pathways, resulting in elevation of cyclin D1, which accelerates the progression of high-grade endometrial stromal sarcoma. Therefore, it was speculated that YWHAE might interact with NUTM2 protein to integrate signaling pathways, and then participate in the progression of BC, which needs to be further explored in follow-up studies.

Notably, circAGFG1 can affect MMP9, GLUT1, and Bax expression in BC cells by targeting and regulating the miR-653-5p/YWHAE axis. MMP9 can degrade matrix proteins, destroy extracellular matrix, and promote tumor cell invasion and metastasis (Augoff *et al*., 2022). In addition, high GLUT1 expression is associated with metabolic reprogramming of tumor cells, including increased glucose uptake, lactic acid production, and acidified microenvironment (Pezzuto *et al*., 2020). Bax activation can increase the permeability of the mitochondrial outer membrane and release apoptosis signaling molecules such as cytochrome C in mitochondria, thus inducing apoptosis (Edlich *et al*., 2018). In this study, we speculate that circAGFG1's function in promoting BC cell invasion and migration is significantly related to the increased expression of MMP9. In addition, circAGFG1 can increase the glycolytic capacity of BC cells by promoting GLUT1 expression, which will provide powerful energy for the proliferation and metastasis of BC cells. The inhibitory effect of circAGFG1 on Bax may reduce the permeability of the mitochondrial membrane of BC cells, thereby preventing the release of apoptosis signaling molecules, which will help to reduce the apoptosis rate of cancer cells.

However, this study is limited in that the effect of circAGFG1 in multiple models of each BC subtype requires further investigation. In addition, the mechanism of YWHAE regulating BC remains to be further explored. Future multicenter trials are required to illustrate circAGFG1's function in BC.

CONCLUSION

Taken together, this study demonstrates that circAGFG1 targeted regulation of YWHAE expression *via* acting as a sponge of miR-653-5p, thereby promoting BC progression. CircAGFG1/miR-653-5p/YWHAE axis may offer as a latent therapeutic target for BC.

REFERENCES

Augoff K, Hryniewicz-Jankowska A, Tabola R, Stach K (2022) MMP9: A tough target for targeted therapy for cancer. *Cancers (Basel)* **14**: https://doi.org/10.3390/cancers14071847

Chu M, Fang Y, Jin Y (2021) CircRNAs as promising biomarker in diagnosis of breast cancer: An updated meta-analysis. *J Clin Lab Anal* **35**: e23934. https://doi.org/10.1002/jcla.23934

Cimino D, Fuso L, Sfiligoi C, Biglia N, Ponzone R, Maggiorotto F, Russo G, Cicatiello L, Weisz A, Taverna D, Sismondi P, De Bortoli M. De Bortoli, M (2008) Identification of new genes associated with breast cancer progression by gene expression analysis of predefined sets of neoplastic tissues. *Int J Cancer* **123**: 1327–1338. https://doi.org/10.1002/ijc.23660

Cui Y, Fan J, Shi W, Zhou Z (2022) Circ_0001667 knockdown blocks cancer progression and attenuates adriamycin resistance by depleting NCOA3 *via* releasing miR-4458 in breast cancer. *Drug Dev Res* **83**: 75–87. https://doi.org/10.1002/ddr.21845

Ding X, Zheng J, Cao M (2021) Circ_0004771 accelerates cell carcinogenic phenotypes *via* suppressing miR-1253-mediated DDAH1 inhibition in breast cancer. *Cancer Manag Res* **13**: 1–11. https://doi.org/10.2147/cmar.s273783

Edlich F (2018) BCL-2 proteins and apoptosis: Recent insights and unknowns. *Biochem Biophys Res Commun* **500**: 26–34. https://doi.org/10.1016/j.bbrc.2017.06.190

Fu B, Liu W, Zhu C, Li P, Wang L, Pan L, Li K, Cai P, Meng M, Wang Y, Zhang A, Tang W, An M (2021) Circular RNA circBCBM1 promotes breast cancer brain metastasis by modulating miR-125a/BRD4 axis. *Int J Biol Sci* **17**: 3104–3117. https://doi.org/10.7150/ijbs.58916

Gong G, She J, Fu D, Zhen D, Zhang B (2021) Circular RNA circ_0084927 regulates proliferation, apoptosis, and invasion of breast cancer cells *via* miR-142-3p/ERC1 pathway. *Am J Transl Res* **13**: 4120–4136

Han W, Wang L, Zhang L, Wang Y, Li Y (2019) Circular RNA circRAD23B promotes cell growth and invasion by miR-593-3p/CCND2 and miR-653-5p/TIAM1 pathways in non-small cell lung cancer. *Biochem Biophys Res Commun* **510**: 462–466. https://doi.org/10.1016/j.bbrc.2019.01.131

He X, Xu T, Hu W, Tan Y, Wang D, Wang Y, Zhao C, Yi Y, Xiong M, Lv W, Wu M, Li X, Wu Y, Zhang Q (2021) Circular RNAs: their role in the pathogenesis and orchestration of breast cancer. *Front Cell Dev Biol* **9**: 647736. https://doi.org/10.3389/fcell.2021.647736

Holmes TR, Al Matouq J, Holmes M, Sioda N, Rudd JC, Bloom C, Nicola L, Palermo NY, Madson JG, Lovas S, Hansen LA (2021) Targeting 14-3-3ε activates apoptotic signaling to prevent cutaneous squamous cell carcinoma. *Carcinogenesis* **42**: 232–242. https://doi.org/10.1093/carcin/bgaa091

Leal MF, Ribeiro HF, Rey JA, Pinto GR, Smith MC, Moreira-Nunes CA, Assumpção PP, Lamarão LM, Calcagno DQ, Montenegro RC, Burbano RR (2016) YWHAE silencing induces cell proliferation, invasion and migration through the up-regulation of CDC25B and MYC in gastric cancer cells: new insights about YWHAE role in the tumor development and metastasis process. *Oncotarget* **7**: 85393–85410. https://doi.org/10.18632/oncotarget.13381

Li C, Peng S, Tang C (2021) MicroRNA-4521 targets hepatoma upregulated protein (HURP) to inhibit the malignant progression of breast cancer. *Bioengineered.* https://doi.org/10.1080/21655979.2021.1996016

Li H, Jin X, Liu B, Zhang P, Chen W, Li Q (2019) CircRNA CBL.11 suppresses cell proliferation by sponging miR-6778-5p in colorectal cancer. *BMC Cancer* **19**: 826. https://doi.org/10.1186/s12885-019-6017-2

Li X, Wang C, Wang S, Hu Y, Jin S, Liu O, Gou R, Nie X, Liu J, Lin B (2021) YWHAE as an HE4 interacting protein can influence the malignant behaviour of ovarian cancer by regulating the PI3K/AKT and MAPK pathways. *Cancer Cell Int* **21**: 302. https://doi.org/10.1186/s12935-021-01989-7

Li Z, Fan H, Chen W, Xiao J, Ma X, Ni P, Xu Z, Yang L (2021) MicroRNA-653-5p promotes gastric cancer proliferation and metastasis by targeting the SOCS6-STAT3 pathway. *Front Mol Biosci* **8**: 655580. https://doi.org/10.3389/fmolb.2021.655580

Liu F, Hu L, Pei Y, Zheng K, Wang W, Li S, Qiu E, Shang G, Zhang J, Zhang X (2020) Long non-coding RNA AFAP1-AS1 accelerates the progression of melanoma by targeting miR-653-5p/RAI14 axis. *BMC Cancer* **20**: 258. https://doi.org/10.1186/s12885-020-6665-2

Liu J, Peng X, Liu Y, Hao R, Zhao R, Zhang L, Zhao F, Liu Q, Liu Y, Qi Y (2021) The diagnostic value of serum exosomal has_circ_0000615 for breast cancer patients. *Int J Gen Med* **14**: 4545–4554. https://doi.org/10.2147/ijgm.s319801

Ma X, Wang C, Chen J, Wei D, Yu F, Sun J (2021) circAGFG1 sponges miR-28-5p to promote non-small-cell lung cancer progression through modulating HIF-1α level. *Open Med (Wars)* **16**: 703–717. https://doi.org/10.1515/med-2021-0269

Ma Y, Niu X, Yan S, Liu Y, Dong R, Li Y (2021) Circular RNA profiling facilitates the diagnosis and prognostic monitoring of breast cancer: A pair-wise meta-analysis. *J Clin Lab Anal* **35**: e23575. https://doi.org/10.1002/jcla.23575

Mashouri L, Yousefi H, Aref AR, Ahadi AM, Molaei F, Alahari SK (2019) Exosomes: composition, biogenesis, and mechanisms in cancer metastasis and drug resistance. *Mol Cancer* **18**: 75. https://doi.org/10.1186/s12943-019-0991-5

Ou WB, Lundberg MZ, Zhu S, Bahri N, Kyriazoglou A, Xu L, Chen T, Mariño-Enriquez A, Fletcher JA (2021) YWHAE-NUTM2 oncoprotein regulates proliferation and cyclin D1 *via* RAF/MAPK and Hippo pathways. *Oncogenesis* **10**: 37. https://doi.org/10.1038/s41389-021-00327-w

Park S, Han SH, Kim HG, Jeong J, Choi M, Kim HY, Kim MG, Park JK, Han JE, Cho GJ, Kim MO, Ryoo ZY, Choi SK (2019) PRPF4 is a novel therapeutic target for the treatment of breast cancer by influencing growth, migration, invasion, and apoptosis of breast cancer cells *via* p38 MAPK signaling pathway. *Mol Cell Probes* **47**: 101440. https://doi.org/10.1016/j.mcp.2019.101440

Pezzuto A, D'Ascanio M, Ricci A, Pagliuca A, Carico E (2020) Expression and role of p16 and GLUT1 in malignant diseases and lung cancer: A review. *Thorac Cancer* **11**: 3060–3070. https://doi.org/10.1111/1759-7714.13651

Qi L, Sun B, Yang B, Lu S (2021) circHIPK3 (hsa_circ_0000284) Promotes proliferation, migration and invasion of breast cancer cells *via* miR-326. *Onco Targets Ther* **14**: 3671–3685. https://doi.org/10.2147/ott.s299190

Qi X, Zhang DH, Wu N, Xiao JH, Wang X, Ma W (2015) ceRNA in cancer: possible functions and clinical implications. *J Med Genet* **52**: 710–718. https://doi.org/10.1136/jmedgenet-2015-103334

Wan L, Han Q, Zhu B, Kong Z, Feng E. 2022) Circ-TFF1 facilitates breast cancer development *via* regulation of miR-338-3p/FGFR1 axis. *Biochem Genet* **60**: 315–335. https://doi.org/10.1007/s10528-021-10102-6

Wang X, Chen M, Fang L (2021) hsa_circ_0068631 promotes breast cancer progression through c-Myc by binding to EIF4A3. *Mol Ther Nucleic Acids* **26**: 122–134. https://doi.org/10.1016/j.omtn.2021.07.003

Wu F, Zhou J (2019) CircAGFG1 promotes cervical cancer progression *via* miR-370-3p/RAF1 signaling. *BMC Cancer* **19**: 1067. https://doi.org/10.1186/s12885-019-6269-x

Wu H, Xu J, Gong G, Zhang Y, Wu S (2021) CircARL8B contributes to the development of breast cancer *via* regulating miR-653-5p/HMGA2 axis. *Biochem Genet* **59**: 1648-1665. https://doi.org/10.1007/s10528-021-10082-7

Wu N, Song H, Ren Y, Tao S, Li S (2020) DGUOK-AS1 promotes cell proliferation in cervical cancer *via* acting as a ceRNA of miR-653-5p. *Cell Biochem Funct* **38**: 870–879. https://doi.org/10.1002/cbf.3506

Wu X, Ren Y, Yao R, Zhou L, Fan R (2021) Circular RNA circMMP11 contributes to lapatinib resistance of breast cancer cells by regulating the miR-153-3p/ANLN Axis. *Front Oncol* **11**: 639961. https://doi.org/10.3389/fonc.2021.639961

Xie H, Wang J, Wang B (2021) Circular RNA Circ_0003221 promotes cervical cancer progression by regulating miR-758-3p/CPEB4 axis. *Cancer Manag Res* **13**: 5337–5350. https://doi.org/10.2147/cmar.s311242

Xie H, Xiao R, He Y, He L, Xie C, Chen J, Hong Y (2021) MicroRNA-100 inhibits breast cancer cell proliferation, invasion and migration by targeting FOXA1. *Oncol Lett* **22**: 816. https://doi.org/10.3892/ol.2021.13077

Yang YF, Lee YC, Wang YY, Wang CH, Hou MF, Yuan SF (2019) YWHAE promotes proliferation, metastasis, and chemoresistance in breast cancer cells. *Kaohsiung J Med Sci* **35**: 408–416. https://doi.org/.1002/kjm2.12075

Zhang C, Liu N (2022) Noncoding RNAs in the glycolysis of ovarian cancer. *Front Pharmacol* **13**: 855488. https://doi.org/10.3389/fphar.2022.855488

Zhang D, Li C, Cheng N, Sun L, Zhou X, Pan G, Zhao J (2021) CircAGFG1 acts as a sponge of miR-4306 to stimulate esophageal cancer progression by modulating MAPRE2 expression. *Acta Histochem* **123**: 151776. https://doi.org/10.1016/j.acthis.2021.151776

Zhang L, Zhang W, Zuo Z, Tang J, Song Y, Cao F, Yu X, Liu S, Cai X (2022) Circ_0008673 regulates breast cancer malignancy by miR-153-3p/CFL2 axis. *Arch Gynecol Obstet* **305**: 223–232. doi:10.1007/s00404-021-06149-w